



Biochar mitigates bioavailability and environmental risks of arsenic in gold mining tailings from the eastern Amazon

Yan Nunes Dias^{a,*}, Wendel Valter da Silveira Pereira^a, Marcela Vieira da Costa^a,
Edna Santos de Souza^b, Silvio Junio Ramos^c, Cristine Bastos do Amarante^d,
Willison Eduardo Oliveira Campos^e, Antonio Rodrigues Fernandes^a

^a Institute of Agricultural Sciences, Federal Rural University of the Amazon, 66077-830, Belém, Pará, Brazil

^b Xingu Institute of Studies, Federal University of Southern and Southeastern Pará, 68380-000, São Félix Do Xingu, Pará, Brazil

^c Vale Institute of Technology – Sustainable Development, 66055-090, Belém, Pará, Brazil

^d Chemical Analysis Laboratory, Emilio Goeldi Museum of Pará, 66077-830, Belém, Pará, Brazil

^e Department of Teaching, Research and Extension, Federal Institute of Amazonas, 69552-555, Tefé, Amazonas, Brazil

ARTICLE INFO

Keywords:

Arsenic contamination
Arsenic bioavailability
Arsenic exposure
Environmental risks

ABSTRACT

Artisanal gold mining has generated tailings highly contaminated by arsenic (As) in Cachoeira do Piriá, eastern Amazon, leading to severe risks to the environment. Such risks should be mitigated considering the bioavailable concentration of the element, since it implies immediate damage to the ecosystem. The objective of this study was to evaluate the potential of biochars in mitigating the environmental risks of bioavailable As concentrations in gold mining tailings from underground and cyanidation exploration. The biochar addition increased mineral components, cation retention, phosphorus in all fractions, and organic and inorganic carbon. The bioavailability of As was reduced after adding the biochars, following the order palm kernel cake biochar > Brazil nut shell biochar > açai seed biochar, with reductions of up to 13 mg kg⁻¹ in the underground mining tailings and 17 mg kg⁻¹ in the cyanidation mining tailings. These results contributed to the statistically significant reduction of the environmental risks in both mining tailings (6–17% in the underground mining tailings and 9–20% in the cyanidation mining tailings), which was emphasized by Pearson's correlation and multivariate analyzes. The incorporation of the bioavailable fractions of As (from sequential extraction) in the environmental risk assessment was a promising method for evaluating the efficiency of biochars in mitigating the damage caused by this metalloid in gold mining tailings.

1. Introduction

Arsenic (As) is the most toxic element according to the Agency for Toxic Substances and Disease Registry (ATSDR, 2017), strongly associated with carcinogenesis in humans (Jaishankar et al., 2014; Singh et al., 2007). The main anthropic source of this metalloid in the environment is mining, due to the exposure of As-rich minerals to weathering (Drahota et al., 2014; Ono et al., 2012; Souza Neto et al., 2020), which can cause heavy environmental contamination, including soils in areas far from the exploration sites, as well as water bodies that could provide water for human consumption and industrial activities (Panagopoulos, 2021a, 2021b; 2021c). This problem is more pronounced in artisanal mining areas, where low mineral recovery techniques are used and the residues are improperly deposited in the environment (Souza Neto et al., 2020).

Total concentrations of potentially toxic elements (PTEs), including As, are usually adopted to assess the risks associated with these elements in contaminated areas. However, this information is not a proper predictor when evaluated individually, due to the fact that it does not reveal the mobility and bioavailability of these contaminants (Adamo et al., 2018; Alan and Kara, 2019; Gope et al., 2017; Nkinahamira et al., 2019). On the other hand, sequential extractions indicate the main fractions in which the PTEs are linked (Gabarrón et al., 2019), allowing to understand the actual risks caused by these elements in contaminated materials (Huang et al., 2016; Jayarathne et al., 2018).

Biochar is a carbonaceous material resulting from the pyrolysis of biomass under low oxygenation, suitable for controlling contamination (Lehmann et al., 2006, 2011; Penido et al., 2019; Uchimiya et al., 2011) and improving soil fertility and biological properties (Bashir et al., 2018;

* Corresponding author.

E-mail address: yan.dias@ufra.edu.br (Y.N. Dias).

<https://doi.org/10.1016/j.jenvman.2022.114840>

Received 29 November 2021; Received in revised form 9 February 2022; Accepted 2 March 2022

Available online 12 March 2022

0301-4797/© 2022 Elsevier Ltd. All rights reserved.

Chen et al., 2020; Liu et al., 2016; Penido et al., 2019; Sun et al., 2020; Wang et al., 2021). Some studies have evaluated the potential of biochar for environmental remediation using sequential extractions, showing how this material affects chemical fractionation, mobility and bioavailability of PTEs (Chen et al., 2020; Huang et al., 2020; L. Lin et al., 2019; Wan et al., 2020; Wang et al., 2020a).

The effects of biochar on the bioavailability of PTEs are related to complexation, adsorption, and precipitation processes promoted by its physicochemical properties (Derakhshan Nejad et al., 2021; Mujtaba Munir et al., 2020; Yuan et al., 2021) and concentrations of metallic ions, such as iron (Fe), manganese (Mn), calcium (Ca) and magnesium (Mg), as well as non-metallic ions, such as phosphorus (P) (Xiang et al., 2020; Xiao et al., 2020; Yin et al., 2021). The application of biochar does not change the total concentrations of PTEs, but rather the bioavailable fraction, which most interacts with the environment (O'Connor et al., 2018; Wang et al., 2021) and threatens the food chain, due to the greater potential for absorption by plants (O'Connor et al., 2018; Peijnenburg, 2020). Thus, our study is a pioneer in assessing the environmental risk of As based on the bioavailable concentrations of this element, in gold mining tailings treated with two biochars never tested before for this purpose.

In Cachoeira do Piriá, northeastern Amazon, different forms of artisanal gold mining have produced tailings highly contaminated by As, which are improperly deposited in the environment and require remediation to protect the ecosystem and local population (Souza Neto et al., 2020). The use of agro-industrial residues (largely produced in the Amazon), in the form of biochar, can be an interesting alternative for the remediation of these tailings, but this has not been studied so far. Therefore, the objectives of this study were: i) to evaluate the effect of biochars on the mobilization of As in two types of gold mining tailings, and ii) to characterize the efficiency of biochars in reducing the environmental risks of As based on the bioavailable concentrations of this metalloid.

2. Material and methods

2.1. Collection of mining wastes

Mining wastes were collected in the municipality of Cachoeira do Piriá, state of Pará, northern Brazil. In this area, mining was carried out by both companies and artisanal workers until 2013, in sites where gold occurs at depths ranging from 40 to 150 m, in quartz veins, vein networks, and shear zones (Mosher, 2013; Santos, 2004). Currently, exploration is performed only by a cooperative through three main ways: i) underground mining, whose tailings have different deposition periods; ii) cyanidation mining, in which underground mining tailings are reprocessed using cyanide; and iii) colluvial mining (Souza Neto et al., 2020).

This study considered two tailings highly contaminated by As (Souza Neto et al., 2020), identified as: i) underground mining tailings, deposited seven years before the collection, from exploration at a depth of approximately 150 m, in which amalgamation is carried out with the conduction of the leachate (solid material and water) on copper plates containing mercury for gold retention, occupying an area greater than 12 ha (Fig. 1S); and ii) cyanidation mining tailings, from recent reprocessing of underground mining tailings with alkaline cyanide solution to complex the residual gold, deposited in area equivalent to 3 ha (Fig. 1S). Both tailings were collected in April 2018, at random to obtain a better representation of each deposition area.

2.2. Production of biochars

Açaí palm (*Euterpe oleracea* Mart.) seeds, Brazil nut (*Bertholletia excelsa* Bonpl.) shells, and palm kernel cake from the processing of oil palm (*Elaeis guineensis* Jacq.) were used in the production of biochars. Açaí seeds and Brazil nut shells were collected at fairs in the

municipality of Belém, state of Pará, where the respective pulp and nuts are processed and sold. Palm kernel cake was collected at a company located in the municipality of Santa Bárbara do Pará, also in the state of Pará. These materials were selected due to the high regional production, varied proportions of lignin, cellulose and hemicellulose, and the potential as adsorbent materials, which is indicated for the remediation of degraded areas (Dias et al., 2019).

These wastes were washed with deionized water and dried in an oven at 50 °C for 24 h. After that, 100 g of each material were weighed, placed in porcelain crucibles, and pyrolyzed in a muffle oven at 700 °C, under a heating rate of 3.33 °C/min. This temperature was adopted due to the generation of biochars with better characteristics and greater adsorption capacity (Dias et al., 2019). The biochars were crushed, sieved (100 mesh), and identified as: B1 - açaí seed biochar; B2 - Brazil nut shell biochar; and B3 - palm kernel cake biochar.

2.3. Characterization of mining tailings and biochars

The concentrations of As in the tailings were extracted according to the EPA 3051A method (USEPA, 2007), in which 9 mL HNO₃ and 3 mL HCl were applied in 0.5 g of each sample, in triplicate, with digestion in a microwave oven (CEM corporation, model MARS 5®). The quantification was carried out using inductively coupled plasma mass spectrometry (ICP-MS, PerkinElmer), including the ERM® CC-141 certified reference material and blank samples to ensure analytical quality. The recovery rate of As was 95%.

The mineralogical characterization (0.15 mm fine fraction) was performed by PANalytical X'PERT PRO MPD (PW 3040/60) diffractometer powder method, with goniometer PW3050/60 (θ/θ), ceramic-ray tubes with Cu (Kα1 = 1.540598 Å), model PW3373/00, long fine focus (2200 W - 60 kV), Kβ nickel filter. The instrumental scanning conditions were: 4°–70°2θ, step size 0.02° 2θ and time/step of 10 s, divergent and automatic slit and anti-spreading of 4°; 10-mm mask; sample in circular motion with frequency of 1 rotation/s for all samples. The materials were identified using X-ray diffraction (Fig. 2S).

In the characterization of biochars, the pH in water was determined at a ratio of 1:10 (solid:solution) (Singh et al., 2017), and the point of zero charge (PZC) was found according to Uchimiya et al. (2011), when the initial and final pH values were equal. The total levels of C, H, N and S were determined using an elemental analyzer (PerkinElmer, model 2400) and the ash content was quantified by combustion of 1 g of biochar in a muffle oven, maintained at 500 °C for 1 h and 700 °C for 2 h (Melo et al., 2013).

The pseudo total concentrations of elements were extracted using the same method used in the characterization of tailings (EPA 3051A) (USEPA, 2007). The analyzes were performed in triplicate, including the ERM® CC-141 certified reference material and blank samples, in order to ensure analytical quality. The recovery rates ranged from 85 to 97%.

2.4. Biochar application experiment

The two artisanal mining tailings were subjected to the application of 5% of biochar. Each treatment (Control, B1, B2 and B3) had five replications, totaling 20 experimental units per tailing, which were conducted in a completely randomized design and maintained at 50% of the total water holding capacity throughout the incubation period, with addition of ultrapure water (Milli-Q).

One year after the addition of biochars, the pseudo total concentrations of Al, Ca, Co, Cu, Fe, K, Mg, Mn, P, S and Zn were quantified by the method EPA 3051A (USEPA, 2007), with recovery rates varying from 87 to 93%. The pH was obtained with a potentiometer in water (1:10 ratio) (Souza et al., 2019) and the cation exchange capacity (CEC) was quantified by the modified method of NH₄-acetate displacement (Yuan et al., 2011). Contents of organic carbon (OC) and inorganic carbon (IC) were determined by loss of mass via dry combustion in a muffle oven, under temperatures of 450 and 950 °C, respectively. Total carbon (TC) was

obtained by the sum of OC and IC (Hussain et al., 2019).

The fractionation of P was performed due to the role that this element plays on the dynamics of As (Xiang et al., 2020; Xiao et al., 2020; Yin et al., 2021). This analysis followed the methodology proposed by He et al. (2014), which allowed to obtain the following fractions: i) soluble inorganic P (P_{sol}), extracted using ultrapure water; ii) labile inorganic P (P_{lab}), extracted using 0.5 M NaHCO_3 ; iii) adsorbed inorganic P (P_{ads}), extracted using 0.1 M NaOH; iv) P associated with minerals (P_{min}), extracted using 1 M HCl; and v) residual P (P_{res}), obtained with acid digestion (method EPA 3051A) of the solid material remaining from the previous extractions. The P_{sol} , P_{lab} , P_{ads} , and P_{min} fractions were quantified by the colorimetric method described by Murphy and Riley (1962), while the P_{res} fraction was quantified using ICP-MS.

2.5. Chemical fractionation of as

The sequential extraction developed by Drahota et al. (2014) was used to study the chemical fractionation of As. This method can be adopted reliably for the partitioning of As in mining wastes, allowing to determine the association of this element with the following fractions: readily soluble (F1); adsorbed (F2); amorphous and poorly-crystalline arsenates, oxides and hydroxosulfates of Fe (F3); well-crystalline arsenates, oxides, and hydroxosulfates of Fe (F4); and sulfides and arsenides (F5).

The F1 fraction was extracted with ultrapure water (1:25 sample: water), stirred for 10 h; the F2 fraction was obtained with 0.01 M $\text{NH}_4\text{H}_2\text{PO}_4$ (1:100 sample:solution), stirred for 16 h; the F3 fraction was extracted with 0.2 M NH_4 -oxalate/oxalic acid (1:100 sample:solution, in the dark, pH 3, stirred for 2 h; the F4 fraction was extracted with 0.2 M NH_4 -oxalate/oxalic acid (1:100 sample:solution, pH 3, at 80 °C), stirred for 4 h; and the F5 fraction was extracted with KCl/HCl/ KHNO_3 solution (1:100 sample:solution). The concentrations were obtained by flame atomic absorption spectrometry (FAAS) (Thermo Scientific, model iCE3000) with a hydride generator (Thermo Scientific, model VP100). To guarantee the analytical quality, these analyzes were performed in triplicate and included a blank sample in each battery. The recovery rate of As was represented by the ratio between the sum of the concentrations found in the F1, F2, F3, F4 and F5 fractions and the total concentration, varying from 92.2 to 97.3%.

2.6. Environmental risk assessment

In this study, the bioavailable concentration (BAC) of As was represented by the soluble and adsorbed fractions (F1 + F2), due to the easier release of the metalloid from these fractions to the ecosystem (Dong et al., 2020; Jayarathne et al., 2018; Silva Júnior et al., 2019). In order to understand the role of biochars in mitigating the environmental risks associated with As in the studied mining tailings, the potential ecological risk index (PERI) was calculated.

The PERI was first proposed by Hakanson (1980), to assess the impact of PTEs on ecosystems considering pseudo total concentrations (Zhang et al., 2018). Although this index has been widely used to study the ecological risk in soils and mining wastes (Kowalska et al., 2018; W. Lin et al., 2019; Pereira et al., 2020; Tapia-Gatica et al., 2020; Xiao et al., 2019), it can overestimate the risks by not considering the bioavailable fraction, which has immediate effect on the ecosystem (O'Connor et al., 2018; Peijnenburg, 2020). Therefore, the bioavailable concentrations were incorporated into the calculation of the modified ecological risk index (PERI_m) according to the methodology proposed by Jayarathne et al. (2018), following equation (1):

$$\text{PERI}_m = T_{As} \times \left(\frac{\text{BAC}_{As}}{\text{NC}_{As}} \right) \quad \text{Equation 1}$$

Where T_{As} is the toxic response factor of As (10) (Hakanson, 1980);

BAC_{As} is the sum of the As concentrations (mg kg^{-1}) in the F1 and F2 fractions (bioavailable fraction); and NC_{As} is the concentration of As in the reference area (2.06 mg kg^{-1}) (Souza Neto et al., 2020). The results were interpreted according to Hakanson (1980), where $\text{PERI} \leq 40$ indicates low risk, $40 < \text{PERI} \leq 80$ indicates moderate risk, $80 < \text{PERI} \leq 160$ indicates considerable risk, $160 < \text{PERI} \leq 320$ indicates high risk, and $320 < \text{PERI}$ indicates very high risk.

2.7. Statistical analyzes

The results were submitted to the Shapiro-Wilk normality test ($p < 0.05$). Given normality, an analysis of variance (ANOVA) was performed and the averages were compared using the Tukey test ($p < 0.05$). Relationships between the properties of the biochars and As fractions in the tailings were evaluated by principal component analysis (PCA) and principal coordinate analysis (PCoA). In addition, to corroborate the results obtained in the PCA and PCoA, Pearson's correlation analysis ($p < 0.05$) was carried out.

A multiple linear regression analysis was performed to generate a robust model for estimating the bioavailability of As. Variables for modeling were selected using Pearson's correlation ($p < 0.05$), while the most appropriate model was selected based on the F test ($p < 0.05$) and AIC (Akaike Information Criterion) values. The equation of the multiple linear regression was obtained by the Stepwise method, eliminating the variables without statistical significance for the model. The precision and accuracy of the selected model were assessed using the coefficient of determination (R^2), adjusted coefficient of determination (R^2 adjusted), and normalized root mean square error (NRMSE) (Waterlot et al., 2016). All statistical analyzes were performed using R, version 4.1.1 (R Core Team, 2021).

3. Results and discussion

3.1. General characteristics of biochars and mining tailings

All biochars studied showed alkaline pH (Table 1), which is related to the accumulation of ash, common in the pyrolysis of organic materials under high temperatures (Adhikari et al., 2019). The ash content had an inverse behavior ($\text{B3} > \text{B1} > \text{B2}$) in relation to the carbon content ($\text{B2} > \text{B1} > \text{B3}$). Biochars with higher ash contents, such as B1 and B3, are rich in inorganic compounds (Domingues et al., 2017) and have lower carbon contents. On the other hand, the lower ash content in B2 is related to the higher carbon content, resulting from the high content of lignin in

Table 1
Characterization of açai seed (B1), Brazil nut shell (B2) and palm kernel cake (B3) biochars.

Property	Biochar		
	B1	B2	B3
pH (in water)	9.70 ± 0.49	9.90 ± 0.50	8.88 ± 0.44
Ash content (%)	4.80 ± 0.11	1.77 ± 0.04	10.19 ± 0.23
Point of zero charge	3.30 ± 0.02	6.75 ± 0.02	5.13 ± 0.02
Al (g kg^{-1})	0.11 ± 0.01	0.11 ± 0.01	0.66 ± 0.03
Ca (g kg^{-1})	1.06 ± 0.02	1.73 ± 0.04	6.3 ± 0.14
Fe (g kg^{-1})	1.01 ± 0.02	2.34 ± 0.02	3.19 ± 0.02
Mg (g kg^{-1})	8.44 ± 0.42	4.29 ± 0.21	51.00 ± 2.55
Mn (g kg^{-1})	0.46 ± 0.01	0.04 ± 0.00	0.428 ± 0.01
S (g kg^{-1})	0.23 ± 0.02	0.35 ± 0.02	0.12 ± 0.02
Soluble P (g kg^{-1})	1.25 ± 0.06	0.33 ± 0.02	3.27 ± 0.16
Labile P (g kg^{-1})	0.16 ± 0.00	0.03 ± 0.00	3.39 ± 0.08
Adsorbed P (g kg^{-1})	0.02 ± 0.02	0.01 ± 0.02	0.70 ± 0.02
Mineral-associated P (g kg^{-1})	0.36 ± 0.02	0.15 ± 0.01	3.05 ± 0.15
Total P (g kg^{-1})	2.03 ± 0.05	0.61 ± 0.01	10.06 ± 0.23
C (%)	79.2 ± 3.96	80.30 ± 4.02	67.22 ± 3.36
H (%)	1.70 ± 0.04	2.22 ± 0.05	1.99 ± 0.05
O (%)	11.60 ± 0.02	14.12 ± 0.02	15.00 ± 0.02
N (%)	1.86 ± 0.02	1.12 ± 0.02	5.60 ± 0.02

the source (Dias et al., 2019).

The biochars presented varied levels of P, Ca, Mg, Mn, Fe and S (Table 1). Such variations can be explained by the different chemical compositions of the materials used as sources (Wang et al., 2021). The fractions of P followed the same trend as the total contents of this element (B3 > B1 > B2). In the environment, P tends to be available after the mineralization of organic material (Wierzbowska et al., 2020), which occurs through pyrolysis in the case of biochars (Adhikari et al., 2019; He et al., 2014).

The pseudo total concentrations of elements were varied in the two gold mining tailings (Table 2), mainly due to the different exploration processes. In both materials, the concentrations of As were extremely higher than the quality reference value (1.4 mg kg^{-1}) established for soils from the state of Pará (Fernandes et al., 2018) and the investigation value (35 mg kg^{-1}) established by the National Environment Council for Brazilian soils (CONAMA, 2009), suggesting potential risks to human health due to As exposure.

The underground mining tailings showed a higher concentration of As when compared to the cyanidation mining tailings, which may be directly related to losses during the dissolution of minerals in cyanidation (Kyle et al., 2012). Such losses can harm the environment and human health due to the contamination of soil, water, and plants (Pereira et al., 2020; Souza Neto et al., 2020). The concentrations found in both tailings are higher than those found by Souza et al. (2017) in Serra Pelada, Brazil, and by Ding et al. (2016) in China.

3.2. Influence of biochars on tailings properties

The addition of biochars increased the concentrations of Co, K, Mn, P and S in the underground mining tailings, as well as Fe, Ca, Cu, K, Mg, Mn, P and S in the cyanidation mining tailings (Table 3). These findings indicate that biochars were relevant sources of inorganic components, which is commonly observed in studies assessing these materials. In a low fertility soil from Nepal, the addition of biochar improved the levels of Ca, Mg, K and P (Pandit et al., 2018). Biochars produced with residues from the southeastern Brazil increased the levels of K and Ca in the soil (Domingues et al., 2017).

The fractionation of P was modified by the application of biochar in both tailings (Table 4). B3 added higher levels of P in all fractions, which is related to the higher total concentrations in this material, followed by B1 and B2 (Table 1). P-rich biomasses, such as palm kernel cake (used in the production of B3), tend to release high levels of this element during pyrolysis (Wang et al., 2021). After the application of biochar, the availability of P is controlled by the biological activity in the environment, in addition to reactions with inorganic colloids (Hosseini et al., 2019; Richardson and Simpson, 2011).

The addition of biochar increased the CEC in the tailings (Table 4), which is related to the negative charges from organic groups (with high reactivity) and alkaline components of ash, increasing the amount of

cation sorption sites (Hailegnaw et al., 2019; Munera-Echeverri et al., 2018). In addition to CEC, the C content also increased with the addition of biochars to the tailings (Table 4), derived from the partial pyrolysis of biomass and carbonates in the ash, as well as the generation of pyrogenic C during the mineralization of OC to IC in pyrolysis (Amoakwah et al., 2020; Dong et al., 2019; Shi et al., 2021). Increase in C with the addition of biochar was also observed by Luo et al. (2020) in soils from China.

3.3. Effects of biochars on as fractionation

3.3.1. Underground mining tailings

All fractions of As were influenced by the biochars, with the exception of the F1 fraction after the addition of B2 (Fig. 1), whose low solubilization potential is related to the lower levels of OC and P (Table 4), resulting in less repulsion of As (Williams et al., 2011; Zheng et al., 2012). On the other hand, the greater solubilization of As with the addition of B1 and B3 is related to the higher contents of ash (Table 1), which is rich in carbonates, hydroxides and oxides, and mineral components (Beiyuan et al., 2017; Dias et al., 2019). Such conditions increased the pH of the tailings (Table 4), favoring the repulsion/solubilization of As oxianions that tend to be easily desorbed (Kim et al., 2018; Tian et al., 2021; Zhang et al., 2020) and replaced by basic components.

The greater solubility of As promoted by B3 in relation to B1 can be explained by the higher levels of P (total and fractions) and OC provided by this biochar (Table 4). In this process, the release of As is from the replacement of this metalloid by P (phosphate ions) on the surface of the tailings particles, due to the chemical similarity between these elements and greater solubilization provided by organic components (Beesley et al., 2014; Lin et al., 2017; Smith and Naidu, 2009; Yin et al., 2017).

The application of B1 and B3 promoted the mobilization of As from the F2, F3 and F4 fractions to the F1 fraction (Fig. 1). These two biochars present higher levels of P (Table 4), which has the potential to replace the electrostatically adsorbed As (Beesley et al., 2014; Lin et al., 2017). Moreover, the dissolved organic matter resulting from the application of these biochars may have caused the dissolution of Fe and Mn oxides (responsible for more stable bonds), releasing the precipitated and adsorbed As (Beiyuan et al., 2017; Kim et al., 2018, 2019, 2020). On the other hand, the dissolution of Fe and Mn oxides may have been lower with the application of B2 due to the lower levels of lignin, producing a lower content of dissolved organic matter (Dias et al., 2019; Kim et al., 2020).

With the addition of B2, the concentrations of As decreased in the F3 fraction and increased in the F5 fraction (Fig. 1), which is due to the dissolution of amorphous minerals (Kim et al., 2018), followed by readsorption in the crystalline fraction, in which As presents greater stability. The higher concentrations of Fe, Co and Mn after application of B2 (Table 3) suggest increased contents of crystalline oxides formed by these elements, causing higher adsorption and lower mobility of As, which has greater stability when bound to oxides (Yin et al., 2017; Yu et al., 2015, 2017). These bonds become stronger and more stable with the aging of the tailings, which decreases solubilization (Agrafioti et al., 2014; Beiyuan et al., 2017; Zhang et al., 2020). B1 was the only biochar that reduced the concentrations of As in the most stable fraction (F5) (Fig. 1), possibly due to the lower levels of Fe in this biochar (Table 1), which may have favored the mobilization of As to less stable fractions.

3.3.2. Cyanidation mining tailings

The application of B1, B2 and B3 reduced the concentrations of As by 15.3, 10.3 and 20.6% in the F2 fraction; 25, 15.3 and 11.1% in the F3 fraction; and 61.6, 24.9 and 19.7% in the F4 fraction, respectively, in relation to the control treatment. Such reductions are directly related to the increment in CEC with the addition of these biochars (Table 4), which increased the electrostatic repulsion of As and favored the mobilization of this metalloid (Lomaglio et al., 2017; Tian et al., 2021; Zhang et al., 2020).

Table 2

Elemental composition of mining wastes before application of biochars.

Element	Mining waste	
	Underground mining tailings	Cyanidation mining tailings
Fe (g kg^{-1})	109.00 ± 2.40	70.20 ± 1.54
Al (mg kg^{-1})	8400.00 ± 453.60	6500.00 ± 351.00
As (mg kg^{-1})	3000.00 ± 162.00	1600.00 ± 86.40
Ca (mg kg^{-1})	1800.00 ± 97.20	4300.00 ± 232.20
Co (mg kg^{-1})	51.00 ± 1.12	49.50 ± 1.09
Cu (mg kg^{-1})	215.00 ± 4.73	83.10 ± 1.83
K (mg kg^{-1})	800.00 ± 12.40	500.00 ± 16.50
Mg (mg kg^{-1})	1700.00 ± 91.80	3200.00 ± 172.80
Mn (mg kg^{-1})	1140.00 ± 61.56	789.00 ± 42.61
P (mg kg^{-1})	330.00 ± 10.89	284.00 ± 6.25
S (mg kg^{-1})	100.00 ± 2.20	200.00 ± 6.60
Zn (mg kg^{-1})	76.00 ± 1.67	48.00 ± 1.06

Table 3

Elemental composition of mining wastes after application of açai seed (B1), Brazil nut shell (B2) and palm kernel cake (B3) biochars.

Element	Underground mining tailings			Cyanidation mining tailings		
	B1	B2	B3	B1	B2	B3
Fe (g kg ⁻¹)	97.60 ± 2.24	100.50 ± 2.31	98.40 ± 2.26	72.10 ± 1.66	68.50 ± 1.58	69.80 ± 1.61
Al (mg kg ⁻¹)	7300.00 ± 379.60	6000.00 ± 312.00	6400.00 ± 332.80	6200.00 ± 322.40	5900.00 ± 306.80	5900.00 ± 306.80
Ca (mg kg ⁻¹)	1600.00 ± 83.20	1700.00 ± 88.40	1700.00 ± 76.35	4500.00 ± 234.00	4300.00 ± 223.60	4100.00 ± 213.20
Co (mg kg ⁻¹)	53.60 ± 1.23	53.90 ± 1.54	50.20 ± 1.15	43.50 ± 1.00	50.90 ± 1.17	48.00 ± 1.10
Cu (mg kg ⁻¹)	189.50 ± 4.36	198.50 ± 4.57	102.50 ± 2.36	88.10 ± 2.03	85.70 ± 1.97	70.50 ± 1.62
K (mg kg ⁻¹)	1000.00 ± 52.00	600.00 ± 21.34	900.00 ± 46.80	800.00 ± 41.60	600.00 ± 31.20	800.00 ± 41.60
Mg (mg kg ⁻¹)	1400.00 ± 72.80	1400.00 ± 68.40	1400.00 ± 72.80	3400.00 ± 176.80	3100.00 ± 161.20	2800.00 ± 145.60
Mn (mg kg ⁻¹)	1120.00 ± 58.24	1160.00 ± 60.32	1100.00 ± 57.20	800.00 ± 41.60	750.00 ± 39.00	742.00 ± 38.58
P (mg kg ⁻¹)	380.00 ± 13.51	330.00 ± 11.73	650.00 ± 33.80	360.00 ± 12.80	290.00 ± 10.31	680.00 ± 35.36
S (mg kg ⁻¹)	200.00 ± 7.11	200.00 ± 4.60	200.00 ± 5.54	500.00 ± 26.00	200.00 ± 4.12	200.00 ± 7.11
Zn (mg kg ⁻¹)	69.00 ± 1.59	72.00 ± 1.66	70.00 ± 1.61	50.00 ± 1.15	47.00 ± 1.08	50.00 ± 1.15

Table 4

Properties of mining wastes after application of açai seed (B1), Brazil nut shell (B2) and palm kernel cake (B3) biochars.

Property	Underground mining tailings				Cyanidation mining tailings			
	Control	B1	B2	B3	Control	B1	B2	B3
pH (in water)	7.07 ± 0.16	7.25 ± 0.27	7.19 ± 0.27	7.33 ± 0.18	8.33 ± 0.21	8.41 ± 0.19	8.27 ± 0.31	8.15 ± 0.28
CEC ^a (cmol _c kg ⁻¹)	37.86 ± 0.95	129.60 ± 5.73	45.00 ± 1.77	47.12 ± 1.86	31.24 ± 0.78	50.77 ± 2.00	46.71 ± 1.84	44.41 ± 1.11
Soluble P (mg kg ⁻¹)	3.61 ± 0.09	17.44 ± 0.69	7.96 ± 0.24	90.17 ± 4.46	6.38 ± 0.19	16.57 ± 0.65	8.79 ± 0.27	80.02 ± 3.96
Labile P (mg kg ⁻¹)	12.93 ± 0.29	24.73 ± 0.88	13.10 ± 0.29	93.48 ± 3.72	17.69 ± 0.40	37.57 ± 1.33	22.87 ± 0.65	142.8 ± 5.68
Adsorbed P (mg kg ⁻¹)	64.90 ± 1.66	85.61 ± 3.06	50.80 ± 1.30	111.70 ± 3.89	55.38 ± 1.42	63.25 ± 1.62	62.42 ± 1.59	108.4 ± 3.88
Mineral P (mg kg ⁻¹)	6.09 ± 0.14	11.89 ± 0.27	7.75 ± 0.17	51.65 ± 2.46	19.14 ± 0.59	28.46 ± 1.36	18.52 ± 0.57	113.8 ± 5.42
Organic C (mg kg ⁻¹)	16.50 ± 0.39	42.50 ± 1.77	38.60 ± 1.61	46.40 ± 1.93	12.2 ± 0.29	41.3 ± 1.72	32.2 ± 1.02	38.5 ± 1.60
Inorganic C (mg kg ⁻¹)	4.60 ± 1.36	4.10 ± 1.21	4.30 ± 1.27	2.70 ± 0.06	20.1 ± 0.98	17.7 ± 0.86	21.1 ± 1.03	17.2 ± 0.84
Total C (mg kg ⁻¹)	21.10 ± 0.54	46.60 ± 2.31	42.90 ± 2.13	49.10 ± 2.44	32.3 ± 1.02	59 ± 2.93	53.3 ± 2.65	55.7 ± 2.77

^a Cation exchange capacity.

The decrease of As concentrations in the F3 and F4 fractions (Fig. 1) with the application of all biochars, especially B1, may be related to the reductive dissolution of Fe and Mn in oxides, caused by the increment in OC, which was more pronounced with the addition of B1 (Table 4) and may have led to the solubilization (Beiyuan et al., 2017; Kim et al., 2018; Wang et al., 2017) and mobilization of As for both less stable (F1 fraction) and more stable (F5 fraction) forms.

The concentrations of As increased in the F5 fraction, corresponding to 38.6, 12.6 and 4% after application of B1, B2 and B3, respectively (Fig. 1). The greater percentage with the addition of B1 is related to the higher concentrations of S, Fe, Ca, Cu and Mn (Table 3), suggesting that greater contents of sulfide compounds tend to favor more stable chemical bonds between As and sulfides (Drahota et al., 2014; Wang et al., 2015). The stabilization of As with the application of biochar was also observed by Luo et al. (2020) in soils from China, as well as by Zhang et al. (2020) in sediments from the same country.

3.4. Multivariate analyzes and Pearson's correlation

In the underground mining tailings, the PCA revealed that the first two principal components (PC) explained 97.2% of the total data variation, with 82.5% explained by PC1 and 14.7% by PC2 (Fig. 2). PC1 was positively dominated by the ash content, total P and fractions, and the F1 fraction of As, indicating that this metalloid is influenced by soluble components (ash) and that there is competition for adsorption sites with phosphate ions, in addition to the dominance of the properties of B3, which promoted greater solubilization of As. Moreover, PC1 was negatively related to CEC, pH, TC and S of B1 and B2, and the F2, F3 and F4 fractions of As. PC2, in turn, was positively dominated by the F5 fraction of As and the contents of S and Fe from biochars, as well as negatively dominated by the concentration of Mn in the biochars, demonstrating the effect of mineral components (Fe, Mn and S) on the retention of As in less available fractions.

Significant Pearson's correlations ($p < 0.05$) were found between the fractions of As and the properties of biochars in the underground mining

tailings (Table 1S), which supports that the addition of these materials modified the bioavailability of the metalloid. The F1 fraction of As showed a positive correlation with ash, Ca, Al, Mn, Mg and P fractions of biochars; the F2, F3 and F4 fractions of As presented negative correlations with ash, Ca, Al, Mn, Mg and P fractions of the biochars; and the F5 fraction of As showed positive correlations with the levels of Fe and Ca in the biochars (Table 1S). Such results indicate that the biochar properties (ash, Ca, Al, Mn, Mg and fractions of P) were essential for the solubilization of As from the most stable fractions (Fig. 1).

The first two principal components accounted for 95.6% of the data variation in the cyanidation mining tailings (Fig. 2), with 77.4% explained by PC1 and 18.2% explained by PC2. PC1 was positively dominated by N, ash, total P and fractions, in addition to the properties of B3, and negatively dominated by CEC, pH, TC, S, and F1 and F2 fractions of As from B1 and B2, due to the greater solubilization caused by the addition of these biochars to the tailings (Fig. 1). PC2 was positively dominated by the F3 and F4 fractions of As and the content of Fe from biochars, and negatively dominated by the F5 fraction of As and the concentration of Mn in the biochars, indicating the influence of mineral components on the retention of As in less reactive fractions.

In the cyanidation mining tailings, the F1 and F2 fractions of As showed negative correlations with ash, Fe, Ca, Al, Mn, Mg and P fractions, as well as positive correlations with pH, CEC and TC of biochars; the F3 and F4 fractions of As showed positive correlations with O, Fe and Ca of biochars; and the F5 fraction of As had negative correlations with Fe, Ca and Al of biochars (Table 1S). These results demonstrate that the changes promoted by the biochar properties (pH, CEC and TC) contributed to the solubilization of As, and that the mineral content (Fe, Ca, Al, Mn and Mg) led to the accumulation of As in less reactive fractions in these materials (Fig. 1).

The models proposed to estimate the bioavailability of As were: i) properties of biochars; ii) properties of mining tailings; and iii) interaction between properties of biochars and mining tailings. The ANOVA revealed that there are no significant differences between the models (Table 2S). The model represented by the interaction between materials

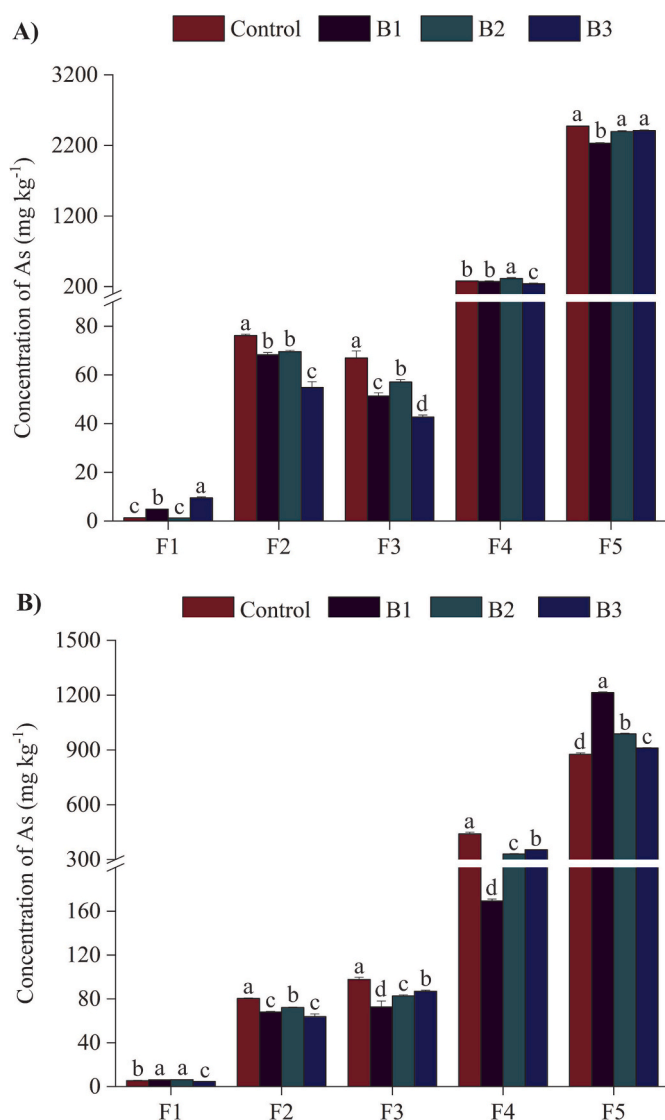


Fig. 1. Concentrations of As in readily-soluble (F1), adsorbed (F2), amorphous and poorly-crystalline arsenates, oxides and hydroxosulfates of Fe (F3), well-crystalline arsenates, oxides, and hydroxosulfates of Fe (F4), and linked to sulfides/arsenides (F5) fractions, in underground mining tailings (A) and cyanidation mining tailings (B) after application of açai seed (B1), Brazil nut shell (B2), and palm kernel cake (B3) biochars. Different letters indicate significant difference between treatments by the Tukey test ($p < 0.05$).

showed higher adjustment values (adjusted R^2) and lower AIC (Table 3S). Therefore, this model was selected as the most representative for multiple linear regression.

The multiple linear regression (Table 4S) revealed that the properties most related to the bioavailability of As were: adsorbed As, total P and fractions (soluble, adsorbed and mineral), and organic carbon in the mining tailings; and ash, CEC, N and P fractions (soluble, adsorbed and mineral) in the biochars. Based on the values of NRMSE and R^2 (Fig. 3S), it is possible to state that the selected model was appropriate for predicting the As bioavailability. All characteristics included in the model ($p < 0.05$) indicate the direct influence of ash (rich in P) and organic compounds (OC and N) in the solubilization of As from stable fractions (Kim et al., 2018, 2020) and, consequently, greater bioavailability. These results suggest that the multiple linear regression can be an important tool, due to the direct influence of the materials on the bioavailability of contaminants (O'Connor et al., 2018; Peijnenburg, 2020).

3.5. Bioavailability and environmental risks of As

The application of biochar decreased the bioavailable concentrations of As in both mining tailings, with results ranging from 64.4 to 77.48 mg kg^{-1} in the underground mining tailings, and from 68.55 to 85.78 mg kg^{-1} in the cyanidation mining tailings (Fig. 4S). These reductions are related to the increase in IC and metal ions such as Al, Fe and Mn (Tables 3 and 4), which contributed to a greater retention of anions in more stable fractions (Wu et al., 2020). The greater bioavailability of As in the cyanidation mining tailings may be related to the use of Na cyanide solution during gold extraction (Kuyucak and Akcil, 2013), which promotes partial dissolution of Fe, Al and Mn minerals (Rubinos et al., 2011), releasing As. After dissolution, the metalloid tends to be even more desorbed with increasing pH, due to competition with OH^- ions (Li et al., 2017; Vodyanitskii, 2006; Xue et al., 2019; Yin et al., 2015).

The bioavailable concentrations of As were incorporated into the assessment of environmental risks to reveal the actual damage of the metalloid. In the control treatment, which indicates the conditions in which tailings are deposited, the PERI_m values were 376.12 in the underground mining tailings and 416.39 in the cyanidation mining tailings (Fig. 3). These results were lower than those obtained by Souza Neto et al. (2020), who studied the environmental risk of As in the same locality, based on pseudo total concentrations, and observed PERI values of 14,131 in the underground mining tailings and 8951 in the cyanidation mining tailings, indicating possible overestimation of risks.

The application of B3 in the underground mining tailings was the only treatment that promoted a change in the class of risk according to the classification proposed by Hakanson (1980) for PERI values, modifying the ecological risk from very high to high (Fig. 3). However, the ecological risk was significantly reduced in all treatments after the application of biochars ($p < 0.05$), with reductions of 5.51, 8.53 and 16.88% in the underground mining tailings, and 13.60, 8.69 and 20.08% in the cyanidation mining tailings, in response to the application of B1, B2 and B3, respectively.

The adoption of bioavailability can be an important tool for the proper assessment of As risk, considering that high bioavailable levels indicate higher mobility and, consequently, greater risk to the environment (Dong et al., 2020; Silva Júnior et al., 2019). In this study, the application of biochars increased the concentrations of As in more stable fractions and decreased the bioavailable level, which is a highly beneficial process for the environment. Moreover, the reduction of the bioavailable fraction and the ecological risk may also imply a reduction in the risk to human health, due to lower As entry into the food chain.

The application of biochar can reduce soil density (Cao et al., 2014) and increase water infiltration into the soil (with increasing porosity), which is fundamental to reduce the dispersion of PTEs (Cao et al., 2014; Chen et al., 2016). On the other hand, biochar can confer less resistance to the soil in relation to external agents, especially in areas of accentuated relief, which are more susceptible to losses by erosion. In these cases, an interesting alternative is the application of biochar together with limestone, which has the potential to improve soil resistance and stability and, consequently, reduce losses by erosive agents (Wang et al., 2020b), protecting water resources for human consumption (Koley, 2021). The adoption of these practices can also promote improvements in soil conditions for plant growth, contributing to increased plant cover and slope stability (Chen et al., 2016).

To better assess the effects of biochars on the environment, it is essential to conduct the new studies involving the bioavailability of As. The application of different rates of biochars under field conditions, including an expressive number of samples and areas, and in different positions in the relief, aiming to have a greater representation of the bioavailable concentrations, to estimate models that can accurately predict the environmental risks of the element (Jia et al., 2021). It would also be interesting to collect organisms (such as plants and fish) to analyze the As content in the issue, aiming to know the content absorbed and bioaccumulated from the environment (Lima et al., 2022; Ray et al.,

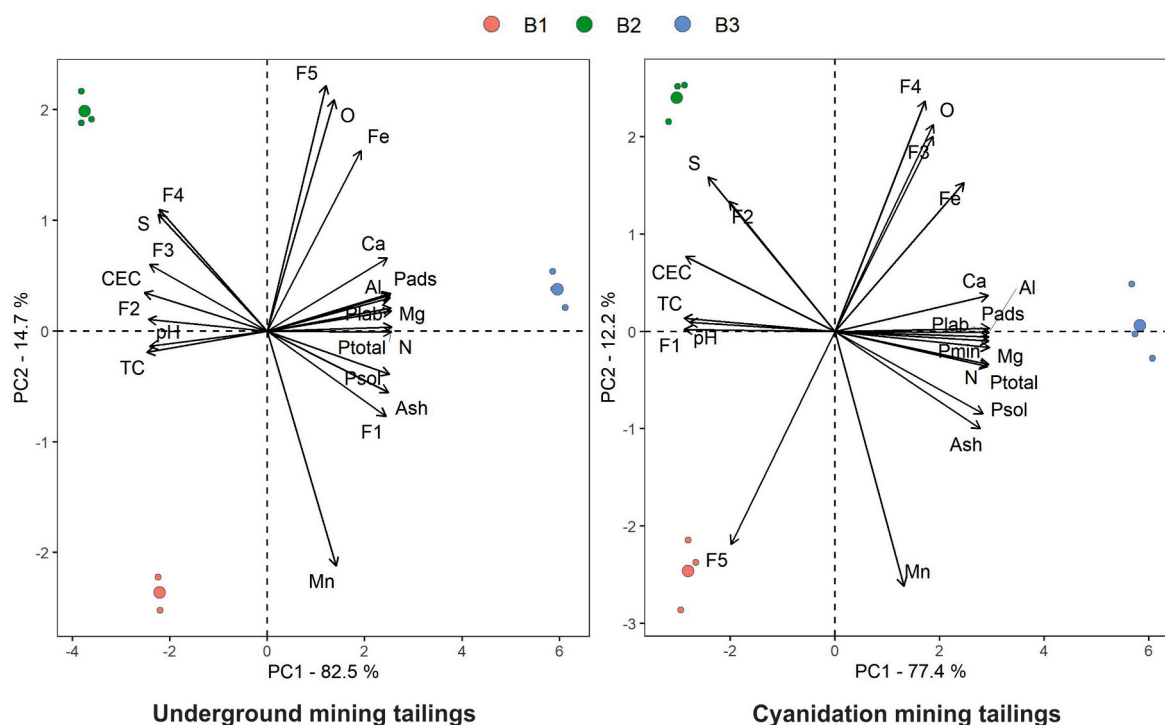


Fig. 2. Principal component analysis between açai seed (B1), Brazil nut shell (B2) and palm kernel cake (B3) biochars and fractions of As in gold mining tailings. (For interpretation of the references to color in this figure legend, the reader is referred to the Web version of this article.)

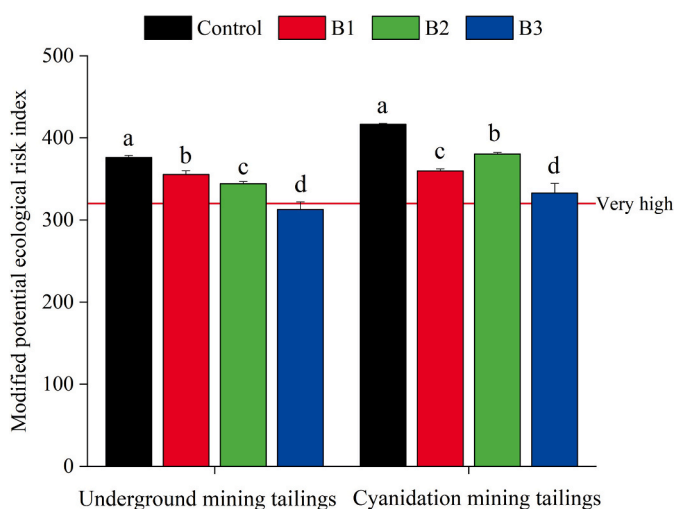


Fig. 3. Potential ecological risk index (PERI_m) modified using bioavailable concentrations of As in gold mining tailings treated with açai seed (B1), Brazil nut shell (B2) and palm kernel cake (B3) biochars. Different letters indicate significant difference between treatments by the Tukey test ($p < 0.05$). (For interpretation of the references to color in this figure legend, the reader is referred to the Web version of this article.)

2021), which could reinforce the role of biochar in reducing the risks to the environment and human health from As exposure.

4. Conclusions

The chemical properties of biochars have a direct influence on the solubility of As in the mining tailings, with emphasis on the levels of P and mineral components, which mobilize the metalloid to less bioavailable fractions. The multivariate (PCA and multiple regression) and Pearson's correlation analyzes demonstrate that the interaction of

biochars with mining tailings is the key to understanding the reduced bioavailability of As. All studied biochars decreased the bioavailable concentrations of As, following the sequence palm kernel cake > Brazil nut shell > açai seed in both tailings, reaching reductions of up to 13 mg kg⁻¹ (underground mining tailings) and 17 mg kg⁻¹ (cyanidation mining tailings). Consequently, the environmental risks decreased between 6 and 17% in the underground mining tailings and between 9 and 20% in the cyanidation mining tailings. The incorporation of the bioavailable concentrations in risk assessments is an alternative for recommending the application of biochars in mining tailings contaminated by As, based on reliable indicators. Our results indicate that the tested biochars can contribute to the mitigation of the impacts caused by As, especially if applied considering the relief conditions and in association with techniques that improve efficiency. In addition, our findings may support new studies focused on the remediation of areas contaminated by As, including the use of new agro-industrial residues and application rates, aiming to reduce the risks to the ecosystem and human health.

Credit author statement

Yan Nunes Dias: Conceptualization, Formal analysis, Methodology, Investigation, Data curation, Writing – original draft, Writing – review & editing. **Wendel Valter da Silveira Pereira:** Conceptualization, Formal analysis, Writing – original draft, Writing – review & editing, Data curation. **Marcela Vieira da Costa:** Investigation, Data curation. **Edna Santos de Souza:** Conceptualization, Writing – review & editing. **Silvio Junio Ramos:** Resources, Conceptualization, Writing – review & editing. **Cristine Bastos do Amarante:** Resources, Data curation. **Willison Eduardo Oliveira Campos:** Investigation. **Antonio Rodrigues Fernandes:** Resources, Funding acquisition, Writing – review & editing, Data curation

Declaration of competing interest

The authors declare that they have no known competing financial interests or personal relationships that could have appeared to influence

the work reported in this paper.

Acknowledgements

The authors would like to thank the Coordination for the Improvement of Higher Education Personnel (CAPES) and the Brazilian National Council for Scientific and Technological Development (CNPq) (No. 425312/2018–6), for the financial support and the scholarships provided in the development of this study.

Appendix A. Supplementary data

Supplementary data to this article can be found online at <https://doi.org/10.1016/j.jenvman.2022.114840>.

References

- Adamo, P., Agrelli, D., Zampella, M., 2018. Chemical speciation to assess bioavailability, bioaccessibility and geochemical forms of potentially toxic metals (PTMs) in polluted soils. In: *Environmental Geochemistry: Site Characterization, Data Analysis and Case Histories*. Elsevier, pp. 153–194. <https://doi.org/10.1016/B978-0-444-63763-5.00010-0>.
- Adhikari, S., Gascó, G., Méndez, A., Surapaneni, A., Jegatheesan, V., Shah, K., Paz-Ferreiro, J., 2019. Influence of pyrolysis parameters on phosphorus fractions of biosolids derived biochar. *Sci. Total Environ.* 695, 133846. <https://doi.org/10.1016/j.scitotenv.2019.133846>.
- Agrafioti, E., Kalderis, D., Diamadopoulos, E., 2014. Ca and Fe modified biochars as adsorbents of arsenic and chromium in aqueous solutions. *J. Environ. Manag.* 146, 444–450. <https://doi.org/10.1016/j.jenvman.2014.07.029>.
- Alan, M., Kara, D., 2019. Assessment of sequential extraction methods for the prediction of bioavailability of elements in plants grown on agricultural soils near to boron mines in Turkey. *Talanta* 200, 41–50. <https://doi.org/10.1016/j.talanta.2019.03.031>.
- Amoakwah, E., Arthur, E., Frimpong, K.A., Parikh, S.J., Islam, R., 2020. Soil organic carbon storage and quality are impacted by corn cob biochar application on a tropical sandy loam. *J. Soils Sediments* 20, 1960–1969. <https://doi.org/10.1007/s11368-019-02547-5>.
- ATSDR, 2017. *Substance Priority List* | ATSDR, Agency for Toxic Substances and Disease Registry.
- Bashir, S., Salam, A., Chhajro, M.A., Fu, Q., Khan, M.J., Zhu, J., Shaaban, M., Kubar, K. A., Ali, U., Hu, H., 2018. Comparative efficiency of rice husk-derived biochar (RHB) and steel slag (SS) on cadmium (Cd) mobility and its uptake by Chinese cabbage in highly contaminated soil. *Int. J. Phytoremediation* 20, 1221–1228. <https://doi.org/10.1080/15226514.2018.1448364>.
- Beesley, L., Inneh, O.S., Norton, G.J., Moreno-Jimenez, E., Pardo, T., Clemente, R., Dawson, J.J.C., 2014. Assessing the influence of compost and biochar amendments on the mobility and toxicity of metals and arsenic in a naturally contaminated mine soil. *Environ. Pollut.* 186, 195–202. <https://doi.org/10.1016/j.envpol.2013.11.026>.
- Beiyuan, J., Awad, Y.M., Beckers, F., Tsang, D.C.W., Ok, Y.S., Rinklebe, J., 2017. Mobility and phytoavailability of As and Pb in a contaminated soil using pine sawdust biochar under systematic change of redox conditions. *Chemosphere* 178, 110–118. <https://doi.org/10.1016/j.chemosphere.2017.03.022>.
- Cao, C.T.N., Farrell, C., Kristiansen, P.E., Rayner, J.P., 2014. Biochar makes green roof substrates lighter and improves water supply to plants. *Ecol. Eng.* 71, 368–374. <https://doi.org/10.1016/j.ecoleng.2014.06.017>.
- Chen, X.-W., Wong, J.T.-F., Ng, C.W.-W., Wong, M.-H., 2016. Feasibility of biochar application on a landfill final cover—a review on balancing ecology and shallow slope stability. *Environ. Sci. Pollut. Res.* 23, 7111–7125. <https://doi.org/10.1007/s11356-015-5520-5>.
- Chen, X., He, H.-Z., Chen, G.-K., Li, H.-S., 2020. Effects of biochar and crop straws on the bioavailability of cadmium in contaminated soil. *Sci. Rep.* 10, 9528. <https://doi.org/10.1038/s41598-020-65631-8>.
- CONAMA, 2009. Resolução Nº 420. Conselho Nacional do Meio Ambiente, Brasília.
- Derakhshan Nejad, Z., Reznia, S., Jung, M.C., Al-Ghamdi, A.A., Mustafa, A.E.-Z.M.A., Elshikh, M.S., 2021. Effects of fine fractions of soil organic, semi-organic, and inorganic amendments on the mitigation of heavy metal(oid)s leaching and bioavailability in a post-mining area. *Chemosphere* 271, 129538. <https://doi.org/10.1016/j.chemosphere.2021.129538>.
- Dias, Y.N., Souza, E.S., da Costa, H.S.C., Melo, L.C.A., Penido, E.S., do Amarante, C.B., Teixeira, O.M.M., Fernandes, A.R., 2019. Biochar produced from Amazonian agro-industrial wastes: properties and adsorbent potential of Cd²⁺ and Cu²⁺. *Biochar* 1, 389–400. <https://doi.org/10.1007/s42773-019-00031-4>.
- Ding, H., Ji, H., Tang, L., Zhang, A., Guo, X., Li, C., Gao, Y., Briki, M., 2016. Heavy metals in the gold mine soil of the upstream area of a metropolitan drinking water source. *Environ. Sci. Pollut. Res.* 23, 2831–2847. <https://doi.org/10.1007/s11356-015-5479-2>.
- Domingues, R.R., Trugilho, P.F., Silva, C.A., de Melo, ICNA, Melo, L.C.A., Magriotes, Z. M., Sánchez-Monedero, M.A., 2017. Properties of biochar derived from wood and high-nutrient biomasses with the aim of agronomic and environmental benefits. *PLoS One* 12, e0176884. <https://doi.org/10.1371/journal.pone.0176884>.
- Dong, H., Xun, Y., Feng, L., Yoneda, M., 2020. Nonlinear transformation and release of arsenic fractions in soil and its implication for site risk assessment. *J. Clean. Prod.* 262, 121304. <https://doi.org/10.1016/j.jclepro.2020.121304>.
- Dong, X., Singh, B.P., Li, G., Lin, Q., Zhao, X., 2019. Biochar increased field soil inorganic carbon content five years after application. *Soil Tillage Res.* 186, 36–41. <https://doi.org/10.1016/j.still.2018.09.013>.
- Drahota, P., Grösslová, Z., Kindlová, H., 2014. Selectivity assessment of an arsenic sequential extraction procedure for evaluating mobility in mine wastes. *Anal. Chim. Acta* 839, 34–43. <https://doi.org/10.1016/j.aca.2014.06.022>.
- Fernandes, A.R., Souza, E.S., de Souza, de, Braz, A.M., Birani, S.M., Alleoni, L.R.F., 2018. Quality reference values and background concentrations of potentially toxic elements in soils from the Eastern Amazon, Brazil. *J. Geochem. Explor.* 190, 453–463. <https://doi.org/10.1016/j.gexplo.2018.04.012>.
- Gabarrón, M., Zornoza, R., Martínez-Martínez, S., Muñoz, V.A., Faz, Á., Acosta, J.A., 2019. Effect of land use and soil properties in the feasibility of two sequential extraction procedures for metals fractionation. *Chemosphere* 218, 266–272. <https://doi.org/10.1016/j.chemosphere.2018.11.114>.
- Gope, M., Mastro, R.E., George, J., Hoque, R.R., Balachandran, S., 2017. Bioavailability and health risk of some potentially toxic elements (Cd, Cu, Pb and Zn) in street dust of Asansol, India. *Ecotoxicol. Environ. Saf.* 138, 231–241. <https://doi.org/10.1016/j.ecoenv.2017.01.008>.
- Hailegnaw, N.S., Mercl, F., Pračke, K., Száková, J., Tlustoš, P., 2019. Mutual relationships of biochar and soil pH, CEC, and exchangeable base cations in a model laboratory experiment. *J. Soils Sediments* 19, 2405–2416. <https://doi.org/10.1007/s11368-019-02264-z>.
- Hakanson, L., 1980. An ecological risk index for aquatic pollution control—a sedimentological approach. *Water Res.* 14 (8), 975–1001. [https://doi.org/10.1016/0043-1354\(80\)90143-8](https://doi.org/10.1016/0043-1354(80)90143-8).
- He, H., Qian, T.-T., Liu, W.-J., Jiang, H., Yu, H.-Q., 2014. Biological and chemical phosphorus solubilization from pyrolytical biochar in aqueous solution. *Chemosphere* 113, 175–181. <https://doi.org/10.1016/j.chemosphere.2014.05.039>.
- Hosseini, S.H., Liang, X., Niyungeko, C., Miaomiao, H., Li, F., Khan, S., Eltohamy, K.M., 2019. Effect of sheep manure-derived biochar on colloidal phosphorus release in soils from various land uses. *Environ. Sci. Pollut. Res.* 26, 36367–36379. <https://doi.org/10.1007/s11356-019-06762-y>.
- Huang, C., Wang, W., Yue, S., Adeel, M., Qiao, Y., 2020. Role of biochar and Eisenia fetida on metal bioavailability and biochar effects on earthworm fitness. *Environ. Pollut.* 263, 114586. <https://doi.org/10.1016/j.envpol.2020.114586>.
- Huang, J., Li, F., Zeng, G., Liu, W., Huang, X., Xiao, Z., Wu, H., Gu, Y., Li, X., He, X., He, Y., 2016. Integrating hierarchical bioavailability and population distribution into potential eco-risk assessment of heavy metals in road dust: a case study in Xiandao District, Changsha city, China. *Sci. Total Environ.* 541, 969–976. <https://doi.org/10.1016/j.scitotenv.2015.09.139>.
- Hussain, S., Sharma, V., Arya, V.M., Sharma, K.R., Rao, C.S., 2019. Total organic and inorganic carbon in soils under different land use/land cover systems in the foothill Himalayas. *Catena* 182, 104104. <https://doi.org/10.1016/j.catena.2019.104104>.
- Jaishankar, M., Tseten, T., Anbalagan, N., Mathew, B.B., Beeregowda, K.N., 2014. Toxicity, mechanism and health effects of some heavy metals. *Interdiscipl. Toxicol.* 7, 60–72. <https://doi.org/10.2478/intox-2014-0009>.
- Jayarathne, A., Egodawatta, P., Ayoko, G.A., Goonetilleke, A., 2018. Assessment of ecological and human health risks of metals in urban road dust based on geochemical fractionation and potential bioavailability. *Sci. Total Environ.* 635, 1609–1619. <https://doi.org/10.1016/j.scitotenv.2018.04.098>.
- Jia, X., Cao, Y., O'Connor, D., Zhu, J., Tsang, D.C.W., Zou, B., Hou, D., 2021. Mapping soil pollution by using drone image recognition and machine learning at an arsenic-contaminated agricultural field. *Environ. Pollut.* 270, 116281. <https://doi.org/10.1016/j.envpol.2020.116281>.
- Kim, H.-B., Kim, J.-G., Choi, J.-H., Kwon, E.E., Baek, K., 2019. Photo-induced redox coupling of dissolved organic matter and iron in biochars and soil system: enhanced mobility of arsenic. *Sci. Total Environ.* 689, 1037–1043. <https://doi.org/10.1016/j.scitotenv.2019.06.478>.
- Kim, H.-B., Kim, J.-G., Kim, T., Alessi, D.S., Baek, K., 2020. Mobility of arsenic in soil amended with biochar derived from biomass with different lignin contents: relationships between lignin content and dissolved organic matter leaching. *Chem. Eng. J.* 393, 124687. <https://doi.org/10.1016/j.cej.2020.124687>.
- Kim, H.-B., Kim, S.-H., Jeon, E.-K., Kim, D.-H., Tsang, D.C.W., Alessi, D.S., Kwon, E.E., Baek, K., 2018. Effect of dissolved organic carbon from sludge, Rice straw and spent coffee ground biochar on the mobility of arsenic in soil. *Sci. Total Environ.* 636, 1241–1248. <https://doi.org/10.1016/j.scitotenv.2018.04.406>.
- Koley, S., 2021. Future perspectives and mitigation strategies towards groundwater arsenic contamination in West Bengal, India. *Environ. Qual. Manag. tqem.* 21784. <https://doi.org/10.1002/tqem.21784>.
- Kowalska, J.B., Mazurek, R., Gasiorek, M., Zaleski, T., 2018. Pollution indices as useful tools for the comprehensive evaluation of the degree of soil contamination - a review. *Environ. Geochem. Health* 40, 2395–2420. <https://doi.org/10.1007/s10653-018-0106-z>.
- Kuyucak, N., Akcil, A., 2013. Cyanide and removal options from effluents in gold mining and metallurgical processes. *Miner. Eng.* 50–51, 13–29. <https://doi.org/10.1016/j.mineng.2013.05.027>.
- Kyle, J.H., Breuer, P.L., Bunney, K.G., Pleysier, R., 2012. Hydrometallurgy review of trace toxic elements (Pb, Cd, Hg, As, Sb, Bi, Se, Te) and their department in gold processing. *Hydrometallurgy* 111–112, 10–21. <https://doi.org/10.1016/j.hydromet.2011.09.005>.
- Lehmann, J., Gaunt, J., Rondon, M., 2006. Bio-char sequestration in terrestrial ecosystems – a review. *Mitig. Adapt. Strategies Glob. Change* 11, 403–427. <https://doi.org/10.1007/s11027-005-9006-5>.

- Lehmann, J., Rillig, M.C., Thies, J., Masiello, C.A., Hockaday, W.C., Crowley, D., 2011. Biochar effects on soil biota – a review. *Soil Biol. Biochem.* 43, 1812–1836. <https://doi.org/10.1016/j.soilbio.2011.04.022>.
- Li, J., Kosugi, T., Riya, S., Hashimoto, Y., Hou, H., Terada, A., Hosomi, M., 2017. Use of batch leaching tests to quantify arsenic release from excavated urban soils with relatively low levels of arsenic. *J. Soils Sediments* 17, 2136–2143. <https://doi.org/10.1007/s11368-017-1669-5>.
- Lima, M.W. de, Pereira, W.V. da S., Souza, E.S. de, Teixeira, R.A., Palheta, D. da C., Faial, K. do C.F., Costa, H.F., Fernandes, A.R., 2022. Bioaccumulation and human health risks of potentially toxic elements in fish species from the southeastern Carajás Mineral Province, Brazil. *Environ. Res.* 204, 112024. <https://doi.org/10.1016/j.envres.2021.112024>.
- Lin, L., Li, Z., Liu, X., Qiu, W., Song, Z., 2019. Effects of Fe-Mn modified biochar composite treatment on the properties of As-polluted paddy soil. *Environ. Pollut.* 244, 600–607. <https://doi.org/10.1016/j.envpol.2018.10.011>.
- Lin, L., Qiu, W., Wang, D., Huang, Q., Song, Z., Chau, H.W., 2017. Arsenic removal in aqueous solution by a novel Fe-Mn modified biochar composite: characterization and mechanism. *Ecotoxicol. Environ. Saf.* 144, 514–521. <https://doi.org/10.1016/j.ecoenv.2017.06.063>.
- Lin, W., Wu, K., Lao, Z., Hu, W., Lin, B., Li, Y., Fan, H., Hu, J., 2019. Assessment of trace metal contamination and ecological risk in the forest ecosystem of dexing mining area in northeast Jiangxi Province, China. *Ecotoxicol. Environ. Saf.* 167, 76–82. <https://doi.org/10.1016/j.ecoenv.2018.10.001>.
- Liu, X., Wang, Y., Gui, C., Li, P., Zhang, J., Zhong, H., Wei, Y., 2016. Chemical forms and risk assessment of heavy metals in sludge-biochar produced by microwave-induced low temperature pyrolysis. *RSC Adv.* 6, 101960–101967. <https://doi.org/10.1039/C6RA22511J>.
- Lomaglio, T., Hattab-Hambli, N., Bret, A., Miard, F., Trupiano, D., Scippa, G.S., Motelica-Heino, M., Bourgerie, S., Morabito, D., 2017. Effect of biochar amendments on the mobility and (bio) availability of As, Sb and Pb in a contaminated mine technosol. *J. Geochem. Explor.* 182, 138–148. <https://doi.org/10.1016/j.jgexplo.2016.08.007>.
- Luo, M., Lin, H., He, Y., Zhang, Y., 2020. The influence of corn-cob-based biochar on remediation of arsenic and cadmium in yellow soil and cinnamon soil. *Sci. Total Environ.* 717, 137014. <https://doi.org/10.1016/j.scitotenv.2020.137014>.
- Melo, L.C.A., Coscione, A.R., Abreu, C.A., Puga, A.P., Camargo, O.A., 2013. Influence of pyrolysis temperature on cadmium and zinc sorption capacity of sugar cane straw-derived biochar. *Bioresources* 8, 4992–5004.
- Mosher, G.Z., 2013. Technical Report and Resource Estimate on the Cachoeira Property. Pará state, Brazil. Vancouver.
- Mujtaba Munir, M.A., Liu, G., Yousaf, B., Ali, M.U., Abbas, Q., Ullah, H., 2020. Synergistic effects of biochar and processed fly ash on bioavailability, transformation and accumulation of heavy metals by maize (*Zea mays* L.) in coal-mining contaminated soil. *Chemosphere* 240, 124845. <https://doi.org/10.1016/j.chemosphere.2019.124845>.
- Munera-Echeverri, J.L., Martinsen, V., Strand, L.T., Zivanovic, V., Cornelissen, G., Mulder, J., 2018. Cation exchange capacity of biochar: an urgent method modification. *Sci. Total Environ.* 642, 190–197. <https://doi.org/10.1016/j.scitotenv.2018.06.017>.
- Murphy, J., Riley, J.P., 1962. A modified single solution method for the determination of phosphate in natural waters. *Anal. Chim. Acta* 27, 31–36. [https://doi.org/10.1016/S0003-2670\(00\)88444-5](https://doi.org/10.1016/S0003-2670(00)88444-5).
- Nkinahamira, F., Suanon, F., Chi, Q., Li, Y., Feng, M., Huang, X., Yu, C.-P., Sun, Q., 2019. Occurrence, geochemical fractionation, and environmental risk assessment of major and trace elements in sewage sludge. *J. Environ. Manag.* 249, 109427. <https://doi.org/10.1016/j.jenvman.2019.109427>.
- O'Connor, D., Peng, T., Zhang, J., Tsang, D.C.W., Alessi, D.S., Shen, Z., Bolan, N.S., Hou, D., 2018. Biochar application for the remediation of heavy metal polluted land: a review of in situ field trials. *Sci. Total Environ.* 619–620, 815–826. <https://doi.org/10.1016/j.scitotenv.2017.11.132>.
- Ono, F.B., Guilherme, L.R.G., Penido, E.S., Carvalho, G.S., Hale, B., Toujaguez, R., Bundschuh, J., 2012. Arsenic bioaccessibility in a gold mining area: a health risk assessment for children. *Environ. Geochem. Health* 34, 457–465. <https://doi.org/10.1007/s10653-011-9444-9>.
- Panagopoulos, A., 2021a. Energetic, economic and environmental assessment of zero liquid discharge (ZLD) brackish water and seawater desalination systems. *Energy Convers. Manag.* 235, 113957. <https://doi.org/10.1016/j.enconman.2021.113957>.
- Panagopoulos, A., 2021b. Techno-economic assessment of minimal liquid discharge (MLD) treatment systems for saline wastewater (brine) management and treatment. *Process Saf. Environ. Protect.* 146, 656–669. <https://doi.org/10.1016/j.psep.2020.12.007>.
- Panagopoulos, A., 2021c. Study and evaluation of the characteristics of saline wastewater (brine) produced by desalination and industrial plants. *Environ. Sci. Pollut. Res.* <https://doi.org/10.1007/s11356-021-17694-x>.
- Pandit, N.R., Mulder, J., Hale, S.E., Martinsen, V., Schmidt, H.P., Cornelissen, G., 2018. Biochar improves maize growth by alleviation of nutrient stress in a moderately acidic low-input Nepalese soil. *Sci. Total Environ.* 625, 1380–1389. <https://doi.org/10.1016/j.scitotenv.2018.01.022>.
- Peijnenburg, W.J.G.M., 2020. Implementation of Bioavailability in Prospective and Retrospective Risk Assessment of Chemicals in Soils and Sediments, pp. 391–422. <https://doi.org/10.1007/978-2020-516>.
- Penido, E.S., Martins, G.C., Mendes, T.B.M., Melo, L.C.A., do Rosário Guimarães, I., Guilherme, L.R.G., 2019. Combining biochar and sewage sludge for immobilization of heavy metals in mining soils. *Ecotoxicol. Environ. Saf.* 172, 326–333. <https://doi.org/10.1016/j.ecoenv.2019.01.110>.
- Pereira, W.V. da S., Teixeira, R.A., Souza, E.S. de, Moraes, A.L.F. de, Campos, W.E.O., Amarante, C.B. do, Martins, G.C., Fernandes, A.R., 2020. Chemical fractionation and bioaccessibility of potentially toxic elements in area of artisanal gold mining in the Amazon. *J. Environ. Manag.* 267, 110644. <https://doi.org/10.1016/j.jenvman.2020.110644>.
- R Core Team, 2021. R: A Language and Environment for Statistical Computing.
- Ray, I., Mridha, D., Roychowdhury, T., 2021. Waste derived amendments and their efficacy in mitigation of arsenic contamination in soil and soil-plant systems: a review. *Environ. Technol. Innovat.* 24, 101976. <https://doi.org/10.1016/j.eti.2021.101976>.
- Richardson, A.E., Simpson, R.J., 2011. Soil microorganisms mediating phosphorus availability update on microbial phosphorus. *Plant Physiol.* 156, 989–996. <https://doi.org/10.1104/pp.111.175448>.
- Rubinos, D.A., Iglesias, L., Díaz-Fierros, F., Barral, M.T., 2011. Interacting effect of pH, phosphate and time on the release of arsenic from polluted river sediments (anllóns river, Spain). *Aquat. Geochem.* 17, 281–306. <https://doi.org/10.1007/s10498-011-9135-2>.
- Santos, Rndoes., 2004. *Investigação do passivo ambiental em Cachoeira do Pirá, NE do Pará: base para a gestão ambiental em áreas garimpadas na Amazônia*. Universidade de São Paulo.
- Shi, S., Zhang, Q., Lou, Y., Du, Z., Wang, Q., Hu, N., Wang, Y., Gunina, A., Song, J., 2021. Soil organic and inorganic carbon sequestration by consecutive biochar application: results from a decade field experiment. *Soil Use Manag.* 37, 95–103. <https://doi.org/10.1111/sum.12655>.
- Silva Júnior, E.C., Martins, G.C., Wadt, L.H.O., Silva, K.E., Lima, R.M.B., Batista, K.D., Guedes, M.C., Oliveira Junior, R.C., Reis, A.R., Lopes, G., Menezes, M.D., Broadley, M.R., Young, S.D., Guilherme, L.R.G., 2019. Natural variation of arsenic fractions in soils of the Brazilian Amazon. *Sci. Total Environ.* 687, 1219–1231. <https://doi.org/10.1016/j.scitotenv.2019.05.446>.
- Singh, B., Arbustain, M.C., Lehmann, J., 2017. *Biochar: A Guide to Analytical Methods*. CRC Press.
- Singh, N., Kumar, D., Sahu, A.P., 2007. Arsenic in the environment: effects on human health and possible prevention. *J. Environ. Biol.* 28, 359–365.
- Smith, E., Naidu, R., 2009. Chemistry of inorganic arsenic in soils: kinetics of arsenic adsorption-desorption. *Environ. Geochem. Health* 31, 49–59. <https://doi.org/10.1007/s10653-008-9228-z>.
- Souza, E.S., Dias, Y.N., Costa, H.S.C., Pinto, D.A., Oliveira, D.M., Souza Falção, N.P., Teixeira, R.A., Fernandes, A.R., 2019. Organic residues and biochar to immobilize potentially toxic elements in soil from a gold mine in the Amazon. *Ecotoxicol. Environ. Saf.* 169, 425–434. <https://doi.org/10.1016/j.ecoenv.2018.11.032>.
- Souza, E.S., Teixeira, R.A., da Costa, H.S.C., Oliveira, F.J., Melo, L.C.A., do Carmo Freitas Faial, K., Fernandes, A.R., 2017. Assessment of risk to human health from simultaneous exposure to multiple contaminants in an artisanal gold mine in Serra Pelada, Pará, Brazil. *Sci. Total Environ.* 576, 683–695. <https://doi.org/10.1016/j.scitotenv.2016.10.133>.
- Souza Neto, H.F. de, Pereira, W.V. da S., Dias, Y.N., Souza, E.S. de, Teixeira, R.A., Lima, M.W. de, Ramos, S.J., Amarante, C.B. do, Fernandes, A.R., 2020. Environmental and human health risks of arsenic in gold mining areas in the eastern Amazon. *Environ. Pollut.* 265, 114969. <https://doi.org/10.1016/j.envpol.2020.114969>.
- Sun, J., Cui, L., Quan, G., Yan, J., Wang, H., Wu, L., 2020. Effects of biochar on heavy metals migration and fractions changes with different soil types in column experiments. *Bioresources* 15, 4388–4406. <https://doi.org/10.15376/biores.15.2.4388-4406>.
- Tapia-Gatica, J., González-Miranda, I., Salgado, E., Bravo, M.A., Tessini, C., Dovletyarova, E.A., Paltseva, A.A., Neaman, A., 2020. Advanced determination of the spatial gradient of human health risk and ecological risk from exposure to As, Cu, Pb, and Zn in soils near the Ventanas Industrial Complex (Puchuncaví, Chile). *Environ. Pollut.* 258, 113488. <https://doi.org/10.1016/j.envpol.2019.113488>.
- Tian, X., Wang, D., Chai, G., Zhang, J., Zhao, X., 2021. Does biochar inhibit the bioavailability and bioaccumulation of As and Cd in co-contaminated soils? A meta-analysis. *Sci. Total Environ.* 762, 143117. <https://doi.org/10.1016/j.scitotenv.2020.143117>.
- Uchimiyama, M., Chang, S., Klasson, K.T., 2011. Screening biochars for heavy metal retention in soil: role of oxygen functional groups. *J. Hazard Mater.* 190, 432–441. <https://doi.org/10.1016/j.jhazmat.2011.03.063>.
- USEPA, 2007. Method 3051A: microwave assisted acid digestion of sediments, sludges, soils, and oils. *Test Methods Eval. Solid Waste*.
- Vodyanitskii, Y.N., 2006. Arsenic, lead, and zinc compounds in contaminated soils according to EXAFS spectroscopic data: a review. *Eurasian Soil Sci.* 39, 611–621. <https://doi.org/10.1134/S1064229306060056>.
- Wan, X., Li, C., Parikh, S.J., 2020. Simultaneous removal of arsenic, cadmium, and lead from soil by iron-modified magnetic biochar. *Environ. Pollut.* 261, 114157. <https://doi.org/10.1016/j.envpol.2020.114157>.
- Wang, J., Shi, L., Zhai, L., Zhang, H., Wang, S., Zou, J., Shen, Z., Lian, C., Chen, Y., 2021. Analysis of the long-term effectiveness of biochar immobilization remediation on heavy metal contaminated soil and the potential environmental factors weakening the remediation effect: a review. *Ecotoxicol. Environ. Saf.* 207, 111261. <https://doi.org/10.1016/j.ecoenv.2020.111261>.
- Wang, N., Xue, X.-M., Juhasz, A.L., Chang, Z.-Z., Li, H.-B., 2017. Biochar increases arsenic release from an anaerobic paddy soil due to enhanced microbial reduction of iron and arsenic. *Environ. Pollut.* 220, 514–522. <https://doi.org/10.1016/j.envpol.2016.09.095>.
- Wang, S., Gao, B., Zimmerman, A.R., Li, Y., Ma, L., Harris, W.G., Migliaccio, K.W., 2015. Removal of arsenic by magnetic biochar prepared from pinewood and natural hematite. *Bioresour. Technol.* 175, 391–395. <https://doi.org/10.1016/j.biortech.2014.10.104>.

- Wang, Yue, Wang, H.-S., Tang, C.-S., Gu, K., Shi, B., 2020b. Remediation of heavy-metal-contaminated soils by biochar: a review. *Environ. Geotech.* 1–14. <https://doi.org/10.1680/jenge.18.00091>.
- Wang, Yi-min, Wang, S., Wang, C., Zhang, Z., Zhang, J., Meng, M., Li, M., Uchimiya, M., Yuan, X., 2020a. Simultaneous immobilization of soil Cd(II) and as(V) by Fe-modified biochar. *Int. J. Environ. Res. Publ. Health* 17, 827. <https://doi.org/10.3390/ijerph17030827>.
- Waterlot, C., Pruvot, C., Bidar, G., Fritsch, C., De Vaulfleur, A., Scheifler, R., Douay, F., 2016. Prediction of extractable Cd, Pb and Zn in contaminated woody habitat soils using a change point detection method. *Pedosphere* 26, 282–298. [https://doi.org/10.1016/S1002-0160\(15\)60043-1](https://doi.org/10.1016/S1002-0160(15)60043-1).
- Wierzbowska, J., Sienkiewicz, S., Żarczyński, P., Krzebietke, S., 2020. Environmental application of ash from incinerated biomass. *Agronomy* 10, 482. <https://doi.org/10.3390/agronomy10040482>.
- Williams, P.N., Zhang, H., Davison, W., Meharg, A.A., Hossain, M., Norton, G.J., Brammer, H., Islam, M.R., 2011. Organic matter—solid phase interactions are critical for predicting arsenic release and plant uptake in Bangladesh paddy soils. *Environ. Sci. Technol.* 45, 6080–6087. <https://doi.org/10.1021/es2003765>.
- Wu, J., Li, Z., Huang, D., Liu, X., Tang, C., Parikh, S.J., Xu, J., 2020. A novel calcium-based magnetic biochar is effective in stabilization of arsenic and cadmium co-contamination in aerobic soils. *J. Hazard Mater.* 387, 122010. <https://doi.org/10.1016/j.jhazmat.2019.122010>.
- Xiang, W., Zhang, X., Chen, J., Zou, W., He, F., Hu, X., Tsang, D.C.W., Ok, Y.S., Gao, B., 2020. Biochar technology in wastewater treatment: a critical review. *Chemosphere* 252, 126539. <https://doi.org/10.1016/j.chemosphere.2020.126539>.
- Xiao, R., Guo, D., Ali, A., Mi, S., Liu, T., Ren, C., Li, R., Zhang, Z., 2019. Accumulation, ecological-health risks assessment, and source apportionment of heavy metals in paddy soils: a case study in Hanzhong, Shaanxi, China. *Environ. Pollut.* 248, 349–357. <https://doi.org/10.1016/j.envpol.2019.02.045>.
- Xiao, Y., Liu, M., Chen, L., Ji, L., Zhao, Z., Wang, L., Wei, L., Zhang, Y., 2020. Growth and elemental uptake of *Trifolium repens* in response to biochar addition, arbuscular mycorrhizal fungi and phosphorus fertilizer applications in low-Cd-polluted soils. *Environ. Pollut.* 260, 113761. <https://doi.org/10.1016/j.envpol.2019.113761>.
- Xue, Q., Ran, Y., Tan, Y., Peacock, C.L., Du, H., 2019. Arsenite and arsenate binding to ferrihydrite organo-mineral coprecipitate: implications for arsenic mobility and fate in natural environments. *Chemosphere* 224, 103–110. <https://doi.org/10.1016/j.chemosphere.2019.02.118>.
- Yin, D., Wang, X., Peng, B., Tan, C., Ma, L.Q., 2017. Effect of biochar and Fe-biochar on Cd and as mobility and transfer in soil-rice system. *Chemosphere* 186, 928–937. <https://doi.org/10.1016/j.chemosphere.2017.07.126>.
- Yin, N., Cui, Y., Zhang, Z., Wang, Z., Cai, X., Wang, J., 2015. Bioaccessibility and dynamic dissolution of arsenic in contaminated soils from Hunan, China. *J. Soils Sediments* 15, 584–593. <https://doi.org/10.1007/s11368-014-1022-1>.
- Yin, Q., Liu, M., Li, Y., Li, H., Wen, Z., 2021. Computational study of phosphate adsorption on Mg/Ca modified biochar structure in aqueous solution. *Chemosphere* 269, 129374. <https://doi.org/10.1016/j.chemosphere.2020.129374>.
- Yu, Z., Qiu, W., Wang, F., Lei, M., Wang, D., Song, Z., 2017. Effects of manganese oxide-modified biochar composites on arsenic speciation and accumulation in an indica rice (*Oryza sativa* L.) cultivar. *Chemosphere* 168, 341–349. <https://doi.org/10.1016/j.chemosphere.2016.10.069>.
- Yu, Z., Zhou, L., Huang, Y., Song, Z., Qiu, W., 2015. Effects of a manganese oxide-modified biochar composite on adsorption of arsenic in red soil. *J. Environ. Manag.* 163, 155–162. <https://doi.org/10.1016/j.jenvman.2015.08.020>.
- Yuan, J.-H., Xu, R.-K., Zhang, H., 2011. The forms of alkalis in the biochar produced from crop residues at different temperatures. *Bioresour. Technol.* 102, 3488–3497. <https://doi.org/10.1016/j.biortech.2010.11.018>.
- Yuan, Y., An, Z., Zhang, R., Wei, X., Lai, B., 2021. Efficiencies and mechanisms of heavy metals adsorption on waste leather-derived high-nitrogen activated carbon. *J. Clean. Prod.* 293, 126215. <https://doi.org/10.1016/j.jclepro.2021.126215>.
- Zhang, P., Qin, C., Hong, X., Kang, G., Qin, M., Yang, D., Pang, B., Li, Y., He, J., Dick, R. P., 2018. Risk assessment and source analysis of soil heavy metal pollution from lower reaches of Yellow River irrigation in China. *Sci. Total Environ.* 633, 1136–1147. <https://doi.org/10.1016/j.scitotenv.2018.03.228>.
- Zhang, W., Tan, X., Gu, Y., Liu, Shaobo, Liu, Y., Hu, X., Li, J., Zhou, Y., Liu, Sijia, He, Y., 2020. Rice waste biochars produced at different pyrolysis temperatures for arsenic and cadmium abatement and detoxification in sediment. *Chemosphere* 250, 126268. <https://doi.org/10.1016/j.chemosphere.2020.126268>.
- Zheng, R.-L., Cai, C., Liang, J.-H., Huang, Q., Chen, Z., Huang, Y.-Z., Arp, H.P.H., Sun, G.-X., 2012. The effects of biochars from rice residue on the formation of iron plaque and the accumulation of Cd, Zn, Pb, as in rice (*Oryza sativa* L.) seedlings. *Chemosphere* 89, 856–862. <https://doi.org/10.1016/j.chemosphere.2012.05.008>.